

# Ignition and Burn Dynamics of DT Fuels in Impact Fast Ignition

Tomoyuki JOHZAKI, Masakatsu MURAKAMI, Hiroshi AZECHI and Kunioki MIMA

*Institute of Laser Engineering, Osaka University, 2-6 Yamada-oka, Suita 565-0871, Japan*

(Received: 29 August 2008 / Accepted: 4 December 2008)

On the basis of 2D hydro-base simulations, where a super-high velocity spherical DT impactor collides against a spherically-compressed stationary DT main fuel, the ignition and burn dynamics in the impact fast ignition (IFI) scheme has been investigated. It is found that the energy conversion from the impactor kinetic energy to its internal energy at the collision is not so high (20 ~ 40 %) since the main fuel is not so hard to completely stop the impactor, which makes ignition requirements harder than that expected at the previous analytical estimation [M. Murakami et al., Nucl. Fusion **46**, 99 (2006)]. And the collision takes a finite time, roughly the impactor length / the impactor velocity, which should be shorter than that the main fuel confinement time. To achieve a high gain in the IFI scheme, the impactor driver energy should be much smaller than that for main fuel implosion, which requires a high compression ( $\geq 100 \text{ g/cm}^3$ ) and a super-high velocity acceleration (2000 ~ 2500 km/sec) for a small mass impactor (less than 10  $\mu\text{g}$ ) before colliding with a main fuel.

Keywords: Impact fast ignition, two-dimensional simulation, ignition and burn dynamics, ignition requirements, DT fusion

## 1. Introduction

In Fast ignition scheme [1], fuel compression and core heating are separately done, which leads to achieving a high gain with about one tenth of the laser energy required in central ignition scheme. In the conventional fast ignition, a compressed core is heated up to the ignition temperature by the energy transport of energetic particles (electrons and/or ions) generated by ultra-intense laser – matter interactions. However, this scheme still has physically un-solved problems such as generation process of energetic particles and the following energy transport. Recently, a new fast ignition scheme – Impact Fast Ignition (IFI) – has been proposed [2], where the imploded main fuel is ignited by impact collision of another imploded fuel (impactor) with super-high velocity, instead of energetic particles. The IFI scheme is physically simpler than the conventional fast ignition scheme using energetic particles for core heating, and also expected to achieve a high gain.

A simple analytical estimation [2], where the kinetic energy of impactor is assumed to be instantaneously and completely converted into its thermal energy at the collision, showed a crucial issue for achieving a high gain in this scheme: simultaneous achievement of the impactor density of  $100 \text{ g/cm}^3$  and velocity of 1000 km/sec. In the first IFI experiments using GEKKO-XII laser system [3], the inflight impactor velocity and density of 640 km/sec and  $0.2 \text{ g/cm}^3$  were demonstrated and the 100 times increase in neutron yield has been observed by the impactor collision.

author's e-mail: tjohzaki@ile.osaka-u.ac.jp

In the present paper, for detailed understanding of the ignition and burn dynamics in the IFI scheme and evaluation of the requirements for ignition and high gain, we carried out two-dimensional (2D) simulations using a burn simulation code FIBMET [4].

## 2. Model Description

The simulation code FIBMET is based on one-fluid and two-temperature Eulerian hydrodynamic code written in 2D cylindrical coordinates ( $r$ - $z$ ) having an axial symmetry. The Quotidian Equation Of State (QEOS) [5] is used for the equation of states. In the energy conservation equation, electron thermal conduction, radiation effects and fusion-products heating are taken into account. The electron thermal conduction is treated by a flux-limited Spitzer–Harm's diffusion model and the radiation transport is treated by a multi-group diffusion model. The radiation processes considered here are bremsstrahlung, inverse-bremsstrahlung and Thomson scattering. For fusion reactions, D-T, D-D (two branches), and D- $^3\text{He}$  reactions are considered. The 3.52-MeV alpha-particle transport is calculated using a multi-group naturally-flux-limited diffusion model [6, 7]. The other charged particles are treated by a simple local/instantaneous deposition model. Neutron heating is neglected.

In Fig.1, the initial conditions for 2D simulations are shown. We assumed a simple situation, *i.e.*, a super-high velocity spherical DT impactor (density  $\rho_s$ , areal density  $\rho R_s$ , temperature  $T_s$ , mass  $M_s$  and velocity  $v_s$ ) collides against a spherically-compressed stationary DT main fuel (density  $\rho_c$ , areal density  $\rho R_c$ , temperature  $T_c$ , and mass

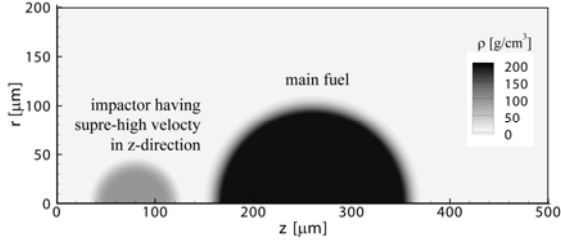


Fig.1 Initial conditions for 2D simulations; cylindrical symmetry is assumed around the horizontal axis ( $z$ -axis).

$M_c$ ). The initial values of the main fuel parameters are fixed in the following simulations;  $\rho_c = 200 \text{ g/cm}^3$ ,  $T_c = 0.17 \text{ keV}$  (the corresponding isentrope parameter  $\alpha_c = 3$ ),  $\rho R_c = 2.0 \text{ g/cm}^2$ ,  $M_c = 850 \text{ μg}$  and internal energy  $E_{ci} = 0.024 \text{ MJ}$ . If the coupling efficiency from the implosion driver energy  $E_{cl}$  to  $E_{ci}$  is assumed as  $\eta_{cl} = 10 \%$ ,  $E_{cl}$  becomes  $0.24 \text{ MJ}$ . As for the impactor, we assumed  $\rho_s = 50 \sim 200 \text{ g/cm}^3$ ,  $\rho R_s = 0.15 \sim 0.8 \text{ g/cm}^2$  and  $v_s = 1000 \sim 3000 \text{ km/sec}$ . The initial value of the impactor temperature is fixed as  $T_s = 0.17 \text{ keV}$ .

### 3. Dynamics of Impactor-Main Fuel Collision

First, we carried out the simulation neglecting fusion reactions to examine the impactor-main fuel collision dynamics.

**Figure 2** shows the temporal evolution of kinetic ( $E_{s(c)k}$ ), internal ( $E_{s(c)i}$ ) and total energies ( $E_{s(c)t}$ ) of the impactor (the main fuel) when an impactor with  $\rho_s = 100 \text{ g/cm}^3$  and  $\rho R_s = 0.4 \text{ g/cm}^2$  collides against the main fuel with the velocity of (a)  $v_s = 1000 \text{ km/sec}$  and (b)  $v_s = 2000 \text{ km/sec}$ . In the case of  $v_s = 1000 \text{ km/sec}$  (2000

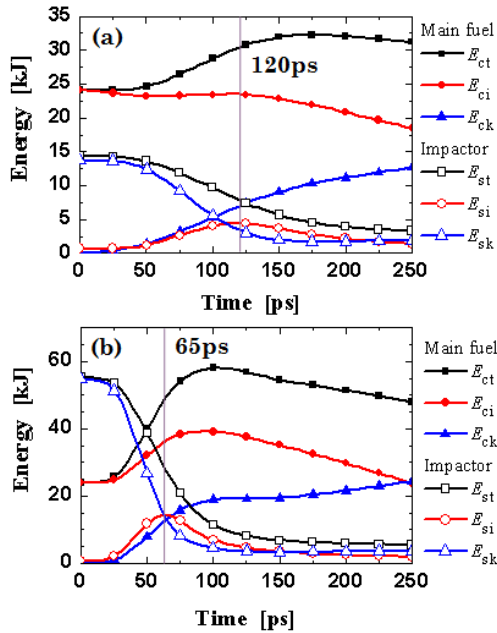


Fig.2 Temporal evolution of kinetic, internal and total energies of impactor and main fuel when the impactor with  $\rho_s = 100 \text{ g/cm}^3$  and  $\rho R_s = 0.4 \text{ g/cm}^2$  collides with the velocity of (a)  $v_s = 1000 \text{ km/sec}$  and (b)  $v_s = 2000 \text{ km/sec}$  against the main fuel.

$\text{km/sec}$ ), the impactor kinetic energy  $E_{sk}$  starts to convert into the internal one  $E_{si}$  at  $t = 40 \text{ ps}$  (20 ps), which means start of the collision, and  $E_{si}$  becomes maximum at  $t = 120 \text{ ps}$  (65 ps); At this moment, the conversion ratio from impactor initial kinetic energy  $E_{sk0}$  to  $E_{si}$ ,  $\eta_{ski}$ , is 32 % (26 %) and the impactor has 25 % (24 %) of  $E_{sk0}$  as the kinetic energy. The other part is transferred into the main fuel. The obtained  $\eta_{ski}$  is far less than 100 % assumed in the simple ignition estimation [2].

In **Fig.3**, we show the one-dimensional (1D) spatial profiles on the central axis ( $r = 0$ ) when  $E_{si}$  becomes maximum for (a)  $v_s = 1000 \text{ km/sec}$  and (b)  $v_s = 2000 \text{ km/sec}$ . It is found that due to the collision, the shock and the reflected shock waves are driven into the main fuel and the impactor, respectively. Note that the impactor penetrates into the main fuel with about a half of its initial velocity since the main fuel with  $\rho_c = 200 \text{ g/cm}^3$  is not so hard to completely stop the impactor with  $\rho_s = 100 \text{ g/cm}^3$ . Due to the collisional compression, the impactor density and temperature increase. In the case of  $v_s = 1000 \text{ km/sec}$ , however, the temperature of impactor reaches only  $1.5 \text{ keV}$ , which is not sufficient for ignition. On the other hand, for  $v_s = 2000 \text{ km/sec}$ , the density and the temperature in the region between the forward shock and the reflected shock reach  $300 \sim 600 \text{ g/cm}^3$  and  $3 \sim 5 \text{ keV}$ . The optical thickness ( $\rho \times \text{thickness}$ ) of the compressed impactor is about  $0.8 \text{ g/cm}^2$ , which corresponds to the hot spot  $\rho R$  of  $0.4 \text{ g/cm}^2$ . These values nearly satisfy the ignition condition.

After the reflected shock passes through the impactor rear edge, the rarefaction wave propagates into the impactor and the impactor density and temperature

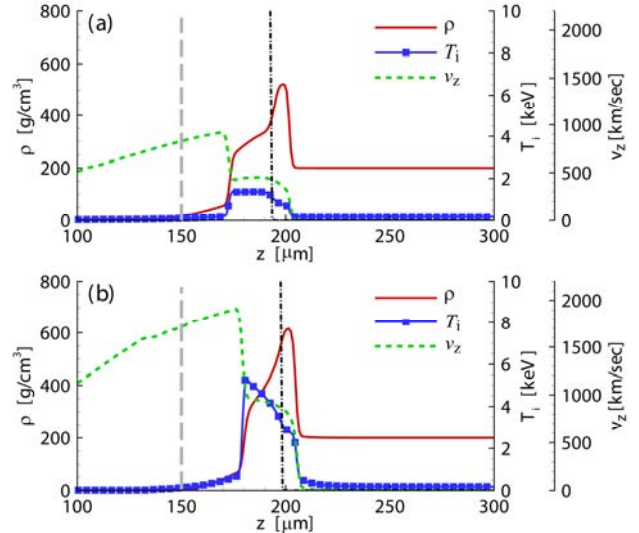


Fig.3 One-dimensional spatial profiles on the central axis ( $r = 0$ ) when  $E_{si}$  becomes maximum for (a)  $v_s = 1000 \text{ km/sec}$  and (b)  $v_s = 2000 \text{ km/sec}$ .  $\rho$ ,  $T_i$  and  $v_z$  stand for mass density, ion temperature and hydro velocity in  $z$ -direction. The dashed-dotted and the long dashed lines indicate the contact surface between main fuel and impactor when  $E_{si}$  becomes maximum and just before collision, respectively.

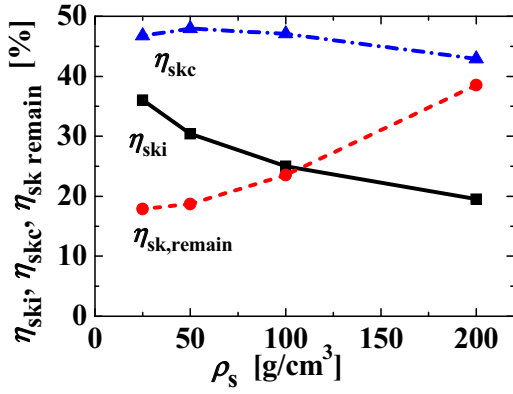


Fig.4 Energy conversion efficiencies when  $E_{si}$  reaches maximum as a function of  $\rho_s$ , where  $R_s$  and  $v_s$  are 40  $\mu\text{m}$  and 2000 km/sec.  $\eta_{ski}$ ,  $\eta_{skc}$  and  $\eta_{skc,remain}$  stand for energy conversion efficiency from impactor kinetic energy to impactor internal energy, energy transfer ratio from impactor kinetic energy to main fuel total energy and the fraction of remaining impactor kinetic energy.

rapidly decrease due to the expansion. Thus, the ignition should take place during a finite collision time from the beginning of collision until the reflected shock passing through the impactor rear edge. This collision time depends on  $v_s$ , the length of impactor and the density ratio between main fuel and impactor, and it should be shorter than the main fuel confinement time, typically several tens  $\sim$  a hundred picoseconds.

We also evaluated the dependence on impactor density, where the impactor radius  $R_s$  and velocity are fixed as  $R_s = 40 \mu\text{m}$  and  $v_s = 2000 \text{ km/sec}$ . In **Fig.4**, the energy conversion efficiencies are plotted as a function of  $\rho_s$ . With decreasing  $\rho_s$ ,  $\rho_c/\rho_s$  becomes large, and then  $\eta_{ski}$  becomes large. The energy transfer rate from the impactor to the main fuel slightly depends on  $\rho_s$ . It ranges from 40 % to 50 %. In **Fig.5**, the 1D spatial profiles on the central axis at  $t = 65 \text{ ps}$  are shown for  $\rho_s = 50 \text{ g/cm}^3$ . Compared with the high density case (Fig.3 (b)), the impactor velocity after collision is small and the temperature is high in the low density case. However, the shock wave driven into the main fuel is weak and the compressed impactor density is low. The optical thickness

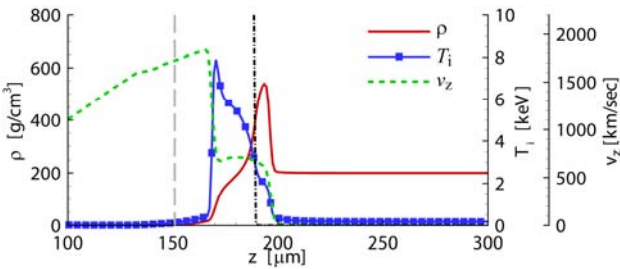


Fig.5 One-dimensional spatial profiles on the central axis ( $r = 0$ ) at  $t = 65 \text{ ps}$  for  $\rho_s = 50 \text{ g/cm}^3$  impactor, where  $R_s$  and  $v_s$  are 40  $\mu\text{m}$  and 2000 km/sec. The notations are the same as in Fig.3.

of impactor after collision is 0.4  $\text{g/cm}^2$ , which corresponds to hot spot  $\rho R$  of 0.2  $\text{g/cm}^2$ .

Since the collisional compression of the impactor is one-dimensional phenomena, the impactor areal density in direction along the collision axis does not change due to the collision. Thus, with decreasing the impactor density, the size of the impactor required for ignition becomes large to keep the hot spot  $\rho R$  required for ignition. As the same time, the collision time is limited by the main fuel confinement time, which requires higher velocity for a lower-density large-size impactor.

#### 4. Ignition and Burn Dynamics in IFI

Next, on the basis of the simulation including fusion reactions, we investigate the ignition and burn dynamics in the IFI scheme and evaluate the requirements for ignition and high gain.

In **Fig.6**, the temporal evolution of DT fusion reaction rate  $R_{DT}$  is shown for  $v_s = 1000$  and 2000 km/sec cases, where  $\rho_s = 100 \text{ g/cm}^3$  and  $\rho R_s = 0.4 \text{ g/cm}^2$ . **Figure 7** shows the temporal evolution of 2D profiles of density, ion temperature and DT fusion reaction rate per unit volume  $r_{DT}$  for the two cases. The impactor outer edge is indicated by the thin white line. When  $v_s = 1000 \text{ km/sec}$ , the slight fusion reactions are observed in the heated impactor at  $t = 50$  and 100 ps, and the shock wave is driven into the main fuel. However, the heating of impactor due to the collision is not sufficient for ignition. The ion temperature in the heated region of impactor is only 1.5 keV. At  $t = 150 \text{ ps}$ , the reflected shock has already passed through the impactor rear edge and the expansion of impactor started, which results in decreasing the density and temperature of impactor before achieving ignition. Thus, the higher impactor velocity is required to heat the impactor up to ignition temperature. In the case of  $v_s = 2000 \text{ km/sec}$ , the collisional compression and heating become stronger and the fusion reaction rate is higher than that in the low velocity case. At  $t = 50 \text{ ps}$ , the fusion reaction takes place

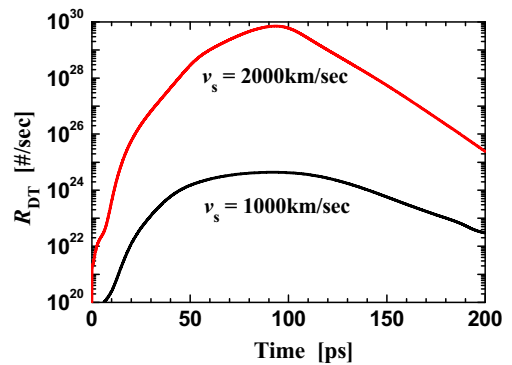


Fig.6 Temporal evolution of DT fusion reaction rate  $R_{DT}$ , is shown for  $v_s = 1000$  and 2000 km/sec cases, where  $\rho_s = 100 \text{ g/cm}^3$  and  $\rho R_s = 0.4 \text{ g/cm}^2$ .

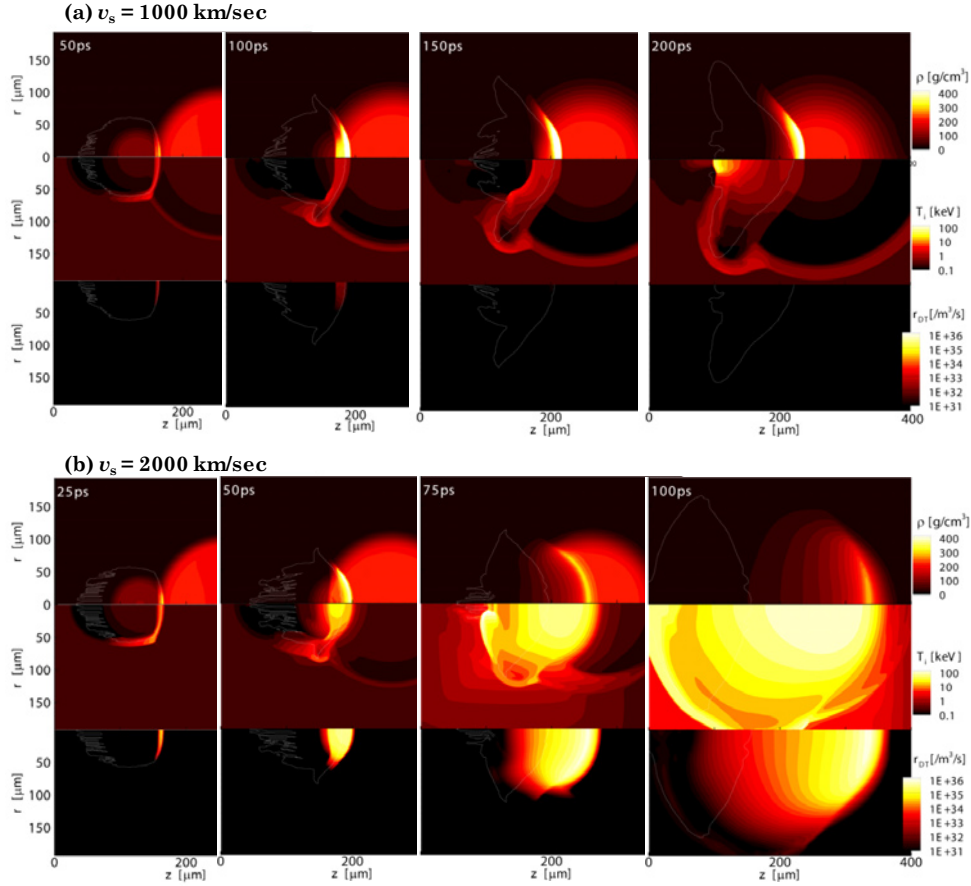


Fig.7 Temporal evolution of two dimensional profiles of density, ion temperature and DT fusion reaction rate per unit volume  $r_{DT}$  for (a)  $v_s = 1000$  and (b)  $2000$  km/sec cases, where  $\rho_s = 100$  g/cm<sup>3</sup> and  $\rho R_s = 0.4$  g/cm<sup>2</sup>.

not only in the impactor region but also in the main fuel region. The temperature in the heated region reaches beyond 10keV, which is higher than that in the case without fusion reactions (Fig.3(b)). Thus, the alpha-particle's self-heating has already worked effectively, which raises the temperature around the collided region further. As the result, before the reflected shock passes through the impactor rear edge, the ignition takes place, and the strong burn wave propagates into the remaining main fuel region. In this case, the fusion output energy of 71.5 MJ is obtained.

To evaluate the threshold impactor velocity required for ignition, we carried out the simulations by varying  $v_s$  from 1000 to 3000km/sec for an impactor with  $\rho_s = 100$  g/cm<sup>3</sup> and  $\rho R_s = 0.4$  g/cm<sup>2</sup>. In Fig.8, the initial impactor kinetic energy  $E_{sk0}$ , the corresponding impactor driver energy  $E_{sL}$  and the obtained fusion output energy are plotted as a function of  $v_s$ , where we assumed a coupling efficiency from the impactor driver energy to the total impactor energy of  $\eta_{sL} = 5\%$ . (The initial internal energy of the impactor is 0.7 kJ, which is negligible compared with  $E_{sk0}$ .) For the impactor with  $\rho_s = 100$  g/cm<sup>3</sup> and  $\rho R_s = 0.4$  g/cm<sup>2</sup>, the ignition threshold velocity is 1750 km/sec and the obtained fusion output energy is 66.2 MJ. The corresponding  $E_{sk0}$  and  $E_{sL}$  are 42 kJ and 0.85 MJ, respectively. The implosion driver energy  $E_{cL}$  is 0.24 MJ

( $\eta_{cL} = 10\%$  is assumed). Then the resultant fusion gain is  $Q = 61$ . Compared with the heating pulse energy in the conventional fast ignition scheme (typically 100 kJ), the impactor driver energy is high. To achieve a high gain such as  $Q \geq 100$  in the IFI scheme, the impactor driver energy should be reduced.

To evaluate the dependence of threshold values of the impactor velocity and kinetic energy on  $\rho_s$  and  $\rho R_s$ , we carried out the parametric simulations. The results are

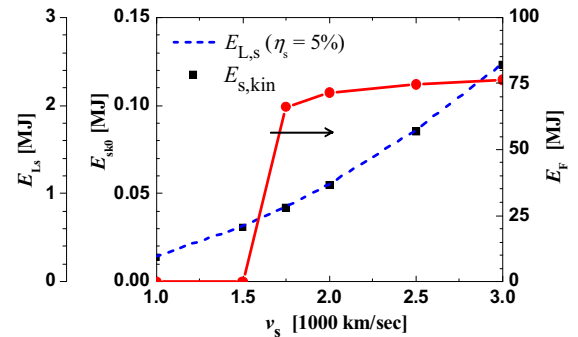


Fig.8 Initial impactor kinetic energy  $E_{sk0}$ , the corresponding impactor driver energy  $E_{sL}$  and the obtained fusion output energy  $E_F$  as a function of  $v_s$ , where the coupling efficiency from the impactor driver energy to the total impactor energy is assumed as  $\eta_{sL} = 5\%$ . The impactor parameters are  $\rho_s = 100$  g/cm<sup>3</sup> and  $\rho R_s = 0.4$  g/cm<sup>2</sup>.



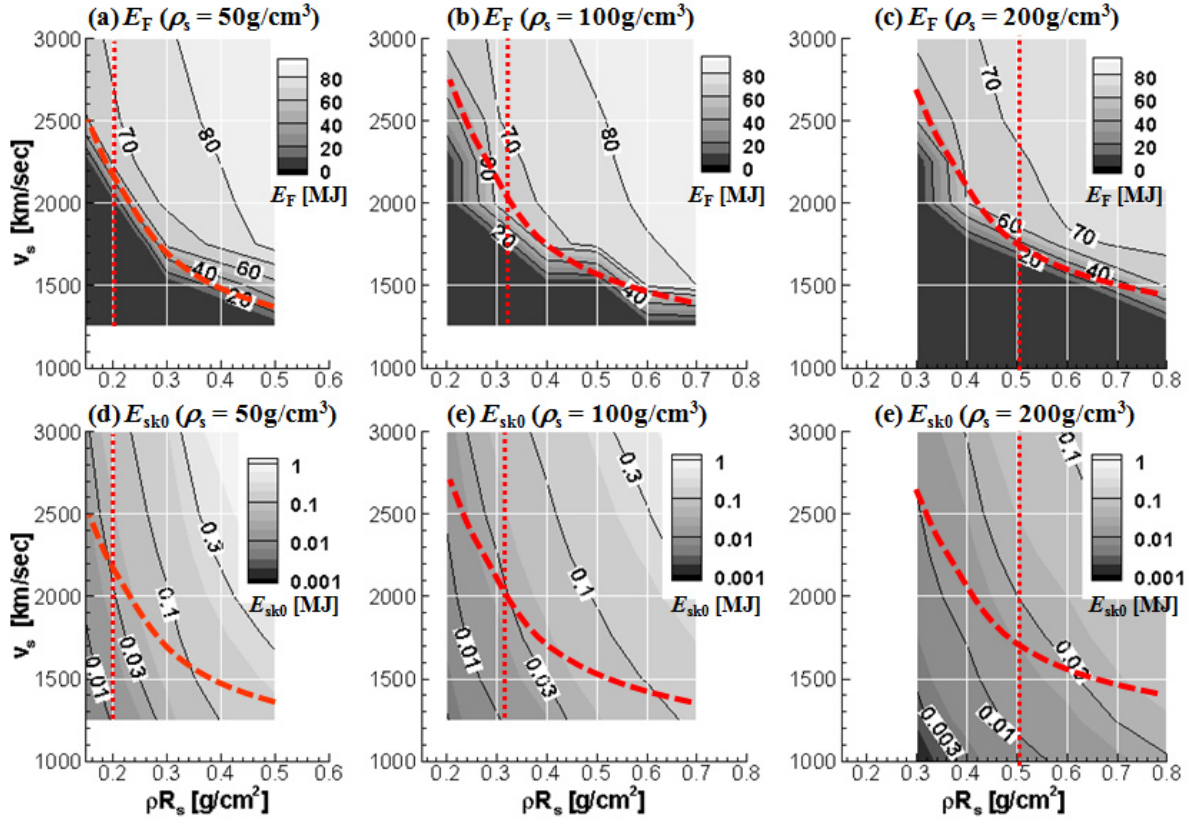


Fig.9 Dependence of threshold values of the impactor velocity and impactor kinetic energy on  $\rho_s$  and  $\rho R_s$ . The thick dashed lines indicate the ignition threshold and the thick dotted lines indicate the impactor mass of  $M_s = 13.4 \mu\text{g}$ .

shown in **Fig.9**. The upper and the lower figures are the contours of fusion output energy and  $E_{sk0}$  as a function of  $v_s$  and  $\rho R_s$  for  $\rho_s = 50, 100, 200 \text{ g/cm}^3$ . The thick dashed lines indicate the ignition threshold.

It can be seen that the threshold velocity for a given  $\rho_s$  becomes higher with decreasing  $\rho R_s$ . In the small  $\rho R_s$  case, the size of the hot spot generated at the collision is also small, which requires high hot spot temperature for ignition. Thus, the higher velocity is required in the smaller  $\rho R_s$  impactor case. On the other hand, the impactor mass is proportional to  $(\rho R_s)^3$ , which contributes to reducing  $E_{sk0}$  with decreasing  $\rho R_s$ . This effect on threshold value of the  $E_{sk0}$  and is larger than the enhancement effect due to increase in threshold velocity, so that the threshold value of the  $E_{sk0}$  and then the  $E_{sL}$  decreases with decreasing  $\rho R_s$ , *e.g.*, when  $\rho R_s$  changes from  $0.8 \text{ g/cm}^2$  to  $0.3 \text{ g/cm}^2$  in the case of  $\rho_s = 200 \text{ g/cm}^3$ , threshold value of  $v_s$  and  $E_{sk0}$  change from  $1500 \text{ km/sec}$  and  $61.5 \text{ kJ}$  to  $2500 \text{ km/sec}$  and  $9.0 \text{ kJ}$ , respectively

For a fixed impactor mass  $M_s$ , the threshold velocity becomes lower with increasing  $\rho_s$ , and the corresponding  $E_{sk0}$  and then the  $E_{sL}$  also decrease because of the large  $\rho R_s$ . For example, in the case of  $M_s = 13.4 \mu\text{g}$  (indicated by thick dotted lines in Fig.9),  $v_s = 2250 \text{ km/sec}$  and  $E_{sk0} = 34.6 \text{ kJ}$  for  $\rho_s = 50 \text{ g/cm}^3$  ( $\rho R_s = 0.2 \text{ g/cm}^2$ ), and  $v_s = 1850 \text{ km/sec}$  and  $E_{sk0} = 26.6 \text{ kJ}$  for  $\rho_s = 200 \text{ g/cm}^3$  ( $\rho R_s = 0.5 \text{ g/cm}^2$ ) are required for ignition, respectively.

Finally, we show the requirement for high gain in the

IFI scheme. In **Fig.10**, the threshold impactor velocity for ignition  $v_{s,thre}$  and the corresponding  $E_{sk0}$  obtained for a given  $\rho R_s$  and  $\rho_s$  are plotted. The lines show the interpolation curves for different  $\rho_s$ . As we showed in Fig.9, higher  $v_{s,thre}$  point corresponds to the impactor with smaller  $\rho R_s$  and  $M_s$ . It is found from Fig.10 that to reduce the impactor energy, not only super-high velocity but also high compression are required. For example, when the  $E_{sL}$  is limited lower than  $200 \text{ kJ}$  and  $\eta_{sL} = 5 \%$  is assumed, the impactor energy should be less than  $10 \text{ kJ}$ . For achieving the ignition under this limited condition,  $v_s \geq 2500$

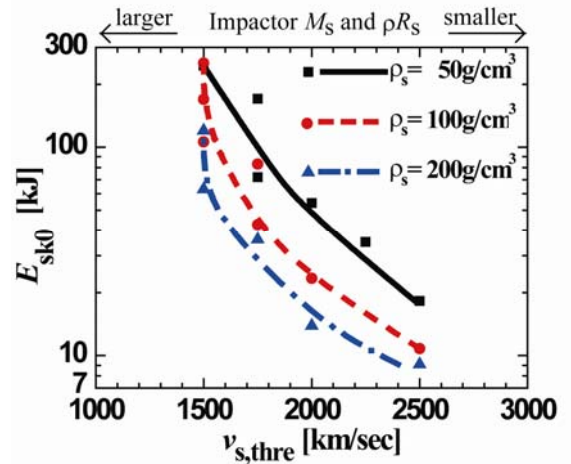


Fig.10 Threshold impactor velocity for ignition  $v_{s,thre}$  and the corresponding  $E_{sk0}$  obtained for a given  $\rho R_s$  and  $\rho_s$ . The lines show the interpolation curves for different  $\rho_s$ .

km/sec and  $\rho_s \geq 100 \text{ g/cm}^3$  are required. When the impactor parameters are  $\rho_s = 200 \text{ g/cm}^3$ ,  $\rho R_s = 0.3 \text{ g/cm}^2$ ,  $v_s = 2500 \text{ km/sec}$  and  $E_{sk0} = 9.0 \text{ kJ}$ , the fusion output energy of  $E_F = 40.2 \text{ MJ}$  is obtained. If  $\eta_{cL} = 10 \%$  and  $\eta_{sL} = 5 \%$  are assumed, the total driver energy and the target gain become  $E_L = 0.42 \text{ kJ}$  and  $Q = 95$ .

## 5. Concluding Remarks

On the basis of 2D hydro-base simulations, where a super-high velocity spherical DT impactor collides against a spherically-compressed stationary DT main fuel, we have investigated the ignition and burn dynamics in the impact fast ignition (IFI).

It is found that the impactor is heated by the reflected shock driven by the collision, so that the heating takes a finite time. This heating time should be sufficiently shorter than the main fuel confinement time to ignite the main fuel. The energy conversion from the impactor kinetic energy to its internal one at the collision increases with the density ratio of the main fuel to the impactor ( $\rho_c / \rho_s$ ). However, it is not as high as that assumed in the simple analytic model [2], where 100 % conversion was assumed, since the main fuel is not so hard to stop the impactor. About a half of impactor kinetic energy is transferred into the main fuel by driving a shock wave. Thus compared with the simple estimation [2], the higher impactor velocity is required to ignite the main fuel.

For a given  $\rho_s$ , the threshold velocity required for ignition becomes higher with decreasing  $\rho R_s$  since the size of the hot spot generated at the collision is small and then the high hot spot temperature is required. However, the impactor mass decreases with  $\rho R_s$ , which reduces the impactor kinetic energy and then the impactor driver energy. For a given mass impactor, the threshold impactor velocity and then the driver energy become smaller with increasing the impactor density because of increase in  $\rho R_s$ . To achieve high gain, the impactor driver energy should be limited to  $E_{sL} = 100 \sim 200 \text{ kJ}$ . If  $E_{sL} = 200 \text{ kJ}$  and the energy coupling from the driver to the impactor is assumed to be 5 % (10 %), a small mass ( $M_s < 4 \text{ } \mu\text{g}$  (10  $\mu\text{g}$ )) impactor required to be compressed up to  $100 \text{ g/cm}^3$ , that is 500 times solid density, and be accelerated up to 2500 km/sec (2000 km/sec) before colliding with a main fuel.

In the present simulation study, we did not discuss the implosion dynamics of main fuel and the acceleration dynamics of impactor in the IFI scheme. Especially, the requirement for impactor shown here seems to be extremely difficult. Further study is required to solve the problem how to achieve the super-high velocity ( $> 2000 \text{ km/sec}$ ) and compression ( $\sim 1000$  times solid density), simultaneously. In addition, the study to reduce the requirement for impactor is required, *e.g.*, the optimization of the impactor and main fuel shapes.

## Acknowledgements

This work was partially supported by the program of the Japan Society of the Promotion of Science under the contract of Grant-in-Aid for Scientific Research (S) No. 18106016. We are grateful for the support of the computer room of ILE and the cybermedia center at Osaka University.

- [1] M. Tabak, J. Hammer, M. E. Glinsky, W. L. Kruer, S. C. Wilks, J. Woodworth, E. M. Campbell, M. D. Perry, and R. J. Mason, *Phys. Plasmas* **1**, 1626 (1994).
- [2] M. Murakami and H. Nagatomo, *Nucl. Inst. Meth. Phys. Res. A* **544**, 67 (2005); M. Murakami, H. Nagatomo, H. Azechi, F. Ogando, M. Perlado and S. Eliezer, *Nucl. Fusion* **46**, 99 (2006).
- [3] H. Azechi, *et al.*, *submitted to Phys. Rev. Lett.*
- [4] T. Johzaki, K. Mima, Y. Nakao, H. Nagatomo, and A. Sunahara, *Proc. International Conference on Inertial Fusion Sciences and Applications, 2003 (IFSA2003)*, Monterey, CA, 2003 (American Nuclear Society, 2004) p.474.
- [5] R. M. More, K. H. Warren, D. A. Young, and G. B. Zimmerman, *Phys. Fluids* **31**(1988)3059.
- [6] C. D. Levermore and G. C. Pomraning, *Astrophys. J.* **248**, 116 (1981).
- [7] T. Johzaki, A. Oda, Y. Nakao, and K. Kudo, *Nucl. Fusion* **39**, 753 (1999).